

NORMALIZING INELASTIC SEISMIC RESPONSE OF STRUCTURES HAVING ECCENTRICITIES IN PLAN

By Michel Bruneau,¹ Associate Member, ASCE,
and Stephen A. Mahin,² Member, ASCE

ABSTRACT: The potentially disastrous consequences of "plan eccentricities" on the seismic response of structures is well recognized, but the exact influence of various parameters on the inelastic response of such systems remains unclear. This paper presents the results of an extensive parametric study conducted to investigate the effect of the uncoupled translational frequency ω_x , the ratio of uncoupled frequencies Ω , the normalized eccentricity (e/r), and the level of excitation, on the inelastic response of simple structures having eccentricities in plan. A procedure is developed to ensure a logical comparison between the response of the eccentric systems and equivalent single-degree-of-freedom (SDOF) benchmark. This procedure hinges on the definition of an equivalent SDOF system, and on a relationship between the excitation levels of the eccentric and SDOF systems. The findings and observations noted from this parametric study, initially conducted on simple monosymmetric bilinear two-element single-story systems, are then shown to be equally applicable for systems with multiple elements, various types of element models, and some simple multistory systems. In consequence of these findings, a simple preliminary design methodology is proposed to estimate ductility demands on simple systems with plan eccentricities, without having to perform detailed inelastic analyses.

INTRODUCTION

When buildings respond inelastically, as is the case during rare and unusually intense earthquakes, their true three-dimensional response may differ significantly from that predicted using conventional elastic analysis methods. This difference can be particularly acute when the distribution of the lateral-load-resisting elements, the mass, or both, results in a noncoincidence between the centers of mass and the centers of stiffness, thus introducing torsional coupling in the plan response. When inelastic response develops, the behavior of such systems can be greatly modified, inducing larger-than-expected demand on some resisting elements. This can lead to excessive local damage to these elements, or even to collapse of the entire structure. Observations of this behavior were made after many major earthquakes, including the Mexican earthquake of September 1985 (Meli 1986; Mitchell et al. 1986). For this earthquake, plan eccentricity was reported to be one of the three major factors responsible for the severe damage or collapse of structures (Meli 1986). Despite numerous observations of this type, a simple method has not been devised to estimate the inelastic response of torsionally coupled systems.

Agnostopoulos et al. (1973), Kan and Chopra (1979), Yamazaki (1980), Tso and Sadek (1984), Syamal and Pekau (1985), and Bozorgnia and Tso (1986), among many others, have studied the inelastic seismic response of torsionally coupled systems, but observations on the effect of various pa-

¹Asst. Prof., Civ. Engrg. Dept., 161 Louis Pasteur, Univ. of Ottawa, Ottawa, Ontario, Canada K1N 6N5.

²Prof. of Civ. Engrg., Univ. of California, Berkeley, CA 94720.

Note. Discussion open until May 1, 1991. To extend the closing date one month, a written request must be filed with the ASCE Manager of Journals. The manuscript for this paper was submitted for review and possible publication on August 2, 1989. This paper is part of the *Journal of Structural Engineering*, Vol. 116, No. 12, December, 1990. ©ASCE, ISSN 0733-9445/90/0012-3358/\$1.00 + \$.15 per page. Paper No. 25359.

parameters on the response of those systems have generally not been in agreement. This can be partly attributed to the diverse analytical assumptions and approaches that were adopted in each study.

A problem germane to the study of torsionally coupled systems is the difficulty in finding a comparative torsion-free "benchmark" system whose response would not be sensitive to any of the parameters thought to influence inelastic torsional response, as well as the difficulty in setting an unbiased liaison between the true system and its benchmark. This paper proposes such a benchmark and liaison, and demonstrates through a parametric study on simple torsionally coupled systems that reasonable parametric independence can be achieved for ductility demands on the resisting elements. More complicated structural systems are then examined to verify that the benchmark and liaison method can be extended to other systems of greater complexity. The utility of this method is demonstrated, based on the availability of inelastic design spectra, to predict the ductility demand of simple torsionally coupled systems. Finally, an example is presented to illustrate the viability of this method.

It should be noted that torsionally coupled inelastic response will also develop following nonsimultaneous yielding of elements in initially symmetric structures. Although such cases of strength eccentricities have also been studied by the writers (Bruneau and Mahin 1987), only the results for plan eccentric structures will be presented herein.

EQUATIONS OF MOTION AROUND CENTER OF MASS

The general equations of motion for single-story torsionally coupled systems are well known and have been derived by others, either around the center of stiffness (Tsicnias and Hutchison 1981) or around the center of mass (Kan and Chopra 1979). For monosymmetric systems (that is, systems having at least one axis of symmetry), the equations along the y -axis (axis of symmetry) are decoupled, and the resulting coupled translational-torsional equations of motion are simplified to

$$\begin{bmatrix} m & 0 \\ 0 & mr^2 \end{bmatrix} \begin{bmatrix} \ddot{v}_x \\ \ddot{v}_\theta \end{bmatrix} + \begin{bmatrix} K_x & -K_x e \\ -K_x e & K_\theta \end{bmatrix} \begin{bmatrix} v_x \\ v_\theta \end{bmatrix} = - \begin{bmatrix} m\ddot{v}_{gx} \\ 0 \end{bmatrix} \dots\dots\dots (1)$$

and, equivalently

$$\begin{bmatrix} \ddot{v}_x \\ r\ddot{v}_\theta \end{bmatrix} + \omega_x^2 \begin{bmatrix} 1 & -e/r \\ -e/r & \Omega^2 \end{bmatrix} \begin{bmatrix} v_x \\ rv_\theta \end{bmatrix} = \begin{bmatrix} -\ddot{v}_{gx} \\ 0 \end{bmatrix} \dots\dots\dots (2)$$

with

$$\Omega = \frac{\omega_\theta}{\omega_x} = \frac{T_x}{T_\theta} \dots\dots\dots (3)$$

$$\omega_x^2 = \frac{K_x}{m} \dots\dots\dots (4)$$

$$\omega_\theta^2 = \frac{K_\theta}{mr^2} \dots\dots\dots (5)$$

where K_x and K_θ = the system's translational (along X) and rotational (around θ) stiffnesses for the resulting two degree-of-freedom system; and e = the

static eccentricity of this system, expressed by

$$K_x = \sum_i K_{ix} \dots\dots\dots (6)$$

$$K_\theta = \sum_i K_{ix}y_i^2 + \sum_j K_{jy}x_j^2 \dots\dots\dots (7)$$

$$e = \frac{1}{K_x} \sum_i y_i K_{ix} \dots\dots\dots (8)$$

where the mass of the floor = m ; its radius of gyration = r ; v_x and \ddot{v}_x = the translational displacement and acceleration of the center of mass in direction x ; v_θ and \ddot{v}_θ = the rotational displacement and acceleration of the floor around a vertical axis; \ddot{v}_{gx} = the ground acceleration in direction x ; y_i and x_j = the distances from element i and j to the center of mass; and K_{ix} and K_{jy} = the translational stiffness of elements i and j in the x - and y -direction, respectively. The translational and torsional uncoupled frequencies, ω_x and ω_θ , the corresponding uncoupled periods, T_x and T_θ , and the ratio of those uncoupled frequencies Ω , are defined in Eqs. 3–5. The torsional stiffness of individual lateral-load-resisting elements is neglected.

Solving Eq. 2, the true natural vibration frequencies can be calculated as

$$\omega_{1,2}^2 = \omega_x^2 \left\{ \frac{(\Omega^2 + 1) \pm \left[\Omega^4 - 2\Omega^2 + 1 + 4\left(\frac{e}{r}\right)^2 \right]^{0.5}}{2} \right\} \dots\dots\dots (9)$$

and

$$\Omega_N^2 = \frac{\omega_N^2}{\omega_x^2}, \text{ for } N = 1, 2 \dots\dots\dots (10)$$

while the resulting mode shapes are

$$\Phi_n = \begin{bmatrix} \Phi_{XN} \\ \Phi_{RN} \end{bmatrix} = \begin{bmatrix} \mathbf{1} \\ (\Omega_N^2 - \mathbf{1})/(\mathbf{e}/r) \end{bmatrix} \dots\dots\dots (11)$$

It is noteworthy that, for large values of Ω , the true first frequency is closer to the uncoupled lateral frequency ω_x , while, for small values of Ω , the true second frequency is closer to the uncoupled lateral frequency ω_x . The two real frequencies are nearly equal only for small eccentricities and when Ω is close to unity. Further, for small Ω , the first mode is subjected to large torsional participation, where for large Ω the translational participation becomes dominant. The opposite occurs for the second mode.

If only two structural elements are provided for the lateral resistance system in the x -direction, the structure is statically determinate, and, in consequence, the lateral shear force must be distributed to the elements solely by the laws of equilibrium. Thus, a static lateral force applied at the center of mass will be distributed to the lateral-load-resisting elements by geometric relations, and independently of their respective stiffnesses. Therefore, in an ideal design process, where the engineer has total control of the structural layout and dimensioning, the resisting elements will be proportioned so that the center of resistance will coincide with the center of mass (unless

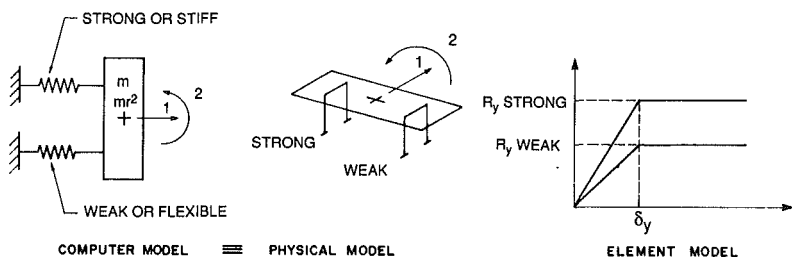


FIG. 1. Element Model Used in Study

the center of mass is not contained between the resisting elements, as would be the case for a building with a single eccentric core). Even so, eccentricities in plan may be introduced by other nonstructural constraints, or when the actual structural behavior differs from that predicted by the simplified design models.

If three (or more) structural elements contribute to the lateral resistance system, many different stiffness distributions can be selected among the resisting elements. If the engineer has unrestrained freedom in the structural design, the centers of mass and stiffness may be made to coincide. However, this may not be possible in many instances, in which case other solutions, also satisfying the equilibrium requirement, will introduce eccentricities in plan between the centers of mass and stiffness.

In this study, simple systems having two lateral-load-resisting elements are used to conduct a comprehensive parametric study. All floor diaphragms are assumed to be infinitely rigid in their own plane. Elements in the orthogonal direction are ignored for the sake of simplicity (i.e., $\sum K_p x_j^2 = 0$). The system studied is illustrated in Fig. 1. Lateral-load-resisting elements are assumed herein to be equidistant from the center of mass. This case has been found to produce larger ductility demand on the edge elements than cases having equal stiffness elements and eccentric center of mass (Bruneau and Mahin 1987). Further, it has been demonstrated elsewhere (Bruneau and Mahin 1987) that the inelastic behavior of simple systems having two lateral-load-resisting elements equidistant from the center of mass can be drastically different than that which would be obtained by either static or dynamic elastic analyses. Those simple systems are thus worthy of serious consideration, and a comprehensive investigation of their behavior is appropriate, especially as findings of such studies can be extended to more elaborate systems, as will be demonstrated later.

INITIALLY ECCENTRIC TWO-ELEMENT SYSTEMS

Determination of Equivalent Single-Degree-of-Freedom (SDOF) System

The importance of defining an equivalent torsion-free system with response that would not be sensitive to any of the parameters thought to influence inelastic torsional response has already been mentioned. Observations of the inelastic behavior of a number of torsionally coupled systems by the writers suggested that this torsion-free benchmark could be adequately defined by a single-degree-of-freedom (SDOF) system having a period equal

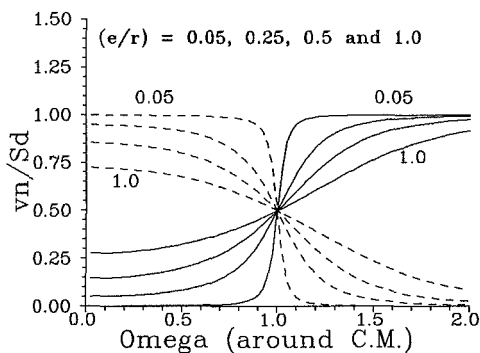


FIG. 2. Participation from each Mode to First Component of Modal Displacement; Solid and Dashed Lines Correspond to First and Second Modes, Respectively

to the predominantly translational period of the torsionally coupled system—that is, the first period of the coupled systems for $\Omega \geq 1.0$, and the second period otherwise (Bruneau and Mahin 1987).

Additional support for this decision is provided by some observations on how modal analysis takes into account the participation of each mode in an elastic torsionally coupled system. From the well-known expression for a component of modal displacement (Clough and Penzien 1975)

$$v_{N,\max} = \left(\frac{\Phi_N L_N}{M_N} \right) S_d(\xi_N, T_N) \dots \dots \dots (12)$$

where $(\Phi_N L_N / M_N)$ = the participation factor for mode N ; $\Phi_N^T = [\Phi_{1N} \ \Phi_{2N}]$ = the components of the N th mode shape; M_N = the generalized mass of the N th normal mode; L_N is the modal earthquake excitation factor for mode N ; and $S_d(\xi_N, T_N)$ = the spectral displacement obtained from a response spectrum for node N , at period T_N and percentage of critical damping ξ_N .

By expanding the participation factor for each mode using the corresponding degree-of-freedom expressions previously defined for torsionally coupled systems, one obtains the following participation factors

$$\frac{\Phi_N L_N}{M_N} = \left[\frac{(\Phi_N L_N / M_N)_1}{(\Phi_N L_N / M_N)_2} \right] = \left[\frac{1/[1 + (\Phi_{2N} / \Phi_{1N})^2]}{1/[(\Phi_{1N} / \Phi_{2N}) + (\Phi_{2N} / \Phi_{1N})]} \right] \dots \dots \dots (13)$$

The edge displacement modal participation factor (EDMPF) for mode N at a distance r from the center of mass (since degrees of freedom at center of mass are v_x and rv_θ) is given by

$$(\text{EDMPF at } r)_N = (\Phi_N L_N / M_N)_1 + (\Phi_N L_N / M_N)_2 \dots \dots \dots (14)$$

Using the mode shape quantities expressed as a function of Ω and (e/r) as presented in Eq. 11, the aforementioned quantities can be calculated. Fig. 2 illustrates the modal participation factor's first component (i.e., corresponding to v_x) with respect to Ω . The second component's effect (corresponding to rv_θ) is plotted in Fig. 3. The EDMPF at distance r is plotted in Fig. 4.

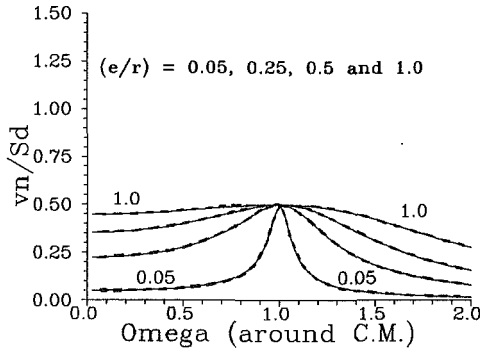


FIG. 3. Participation from each Mode to Second Component of Modal Displacement; Solid and Dashed Lines Correspond to First and Second Modes, Respectively

The final response will clearly depend on the respective values of the spectral displacements S_d appropriate for each mode. Nevertheless, as demonstrated by Fig. 4, and for S_d not too dissimilar for each mode, the response will be primarily affected by a single vibration mode, except in the neighborhood of $\Omega = 1.0$. The dominant mode is apparently the primarily translational one (i.e., the first mode when $\Omega > 1.0$ and the second one when $\Omega < 1.0$).

These observations, as well as analytical developments for the special case $\Omega = 1.0$ (Bruneau and Mahin 1987) not presented here for brevity, lead to the decision to set the equivalent SDOF system's period equal to the first mode of the torsionally coupled system when $\Omega \geq 1.0$, and to the second mode when $\Omega < 1.0$.

Many nonlinear time history analyses were performed, and results were plotted for various combinations of T_x , Ω and e/r to assess the validity of this decision. By comparing torsionally coupled displacement histories with

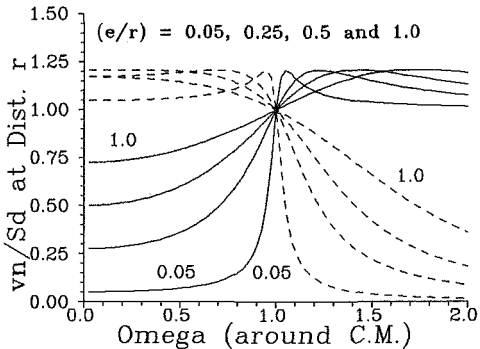


FIG. 4. Participation from each Mode to Displacement at Distance r from Center of Mass; Solid and Dashed Lines Correspond to First and Second Modes, Respectively

those for the equivalent SDOF system, in accordance with an amplitude scaling method to be described in the following sections, the choice of period for the equivalent SDOF system was found appropriate, providing, in most cases, a response history curve for the equivalent SDOF system that closely resembled the one for the elements in the torsionally coupled system. Examples of these time histories are presented elsewhere (Bruneau and Mahin 1987).

Nonlinear Analyses of Torsionally Coupled Systems—Parametric Study

A parametric study was performed to establish a relationship between equivalent SDOF systems' ductility and the element ductilities in torsionally coupled systems; in particular, the effects of various parameters on torsionally coupled elements' response were investigated when equivalent SDOF systems achieved preselected target ductility values.

For this parametric study, simple bilinear inelastic element models were chosen to represent the two-element structure shown in Fig. 1. The introduction of more sophisticated modeling was not warranted at this stage, but due consideration will be given to other nonlinear element models in a subsequent section. Strain hardening was set to 0.5% of the initial elastic stiffness of the elements, making the element model almost elasto-perfectly plastic. Elements of the torsionally coupled system were modeled to have the same yield displacements δ_y (Fig. 1). The damping was chosen to be of the Rayleigh type, arbitrarily set at 2% of the critical damping for each of the true elastic frequencies of the systems analyzed. The study was performed for 10 values of uncoupled period T_x (0.1, 0.2, 0.3, 0.4, 0.6, 0.8, 1.0, 1.2, 1.6, and 2.0 s), six values of the ratio of uncoupled frequencies Ω (0.4, 0.8, 1.0, 1.2, 1.6, and 2.0), two target ductility levels μ_T (4 and 8), and two normalized eccentricities (e/r) (0.1 and 0.3).

To provide results mostly independent of the particular characteristics of a single earthquake, five different earthquake records (El Centro 1940 N-S, Olympia 1949 N-S, Parkfield 1966 S16E, Paicoma Dam 1971 N65E, and Taft 1952 N21E) were considered, and the mean, and mean-plus-one standard deviation, of response values were calculated.

To understand the sensitivity of response to the parameters considered, a liaison between the true systems and benchmark SDOF systems was developed, as described herein. This relates the response of the SDOF inelastic model to that of a multiple-degree-of-freedom model through a transformation function based on elastic response.

1. Equivalent SDOF systems were defined to have a period equal to the first period of their corresponding torsionally coupled system when $\Omega \geq 1.0$, and equal to the second period when $\Omega < 1.0$, as described previously. These SDOF systems were designed so that they shared the same hysteretic characteristics and same yield displacement δ_y as the elements of the torsionally coupled systems.

2. Normalized strength factors necessary for each SDOF system to attain target ductilities μ_T of 4 and 8 were calculated for each earthquake record, using the program NONSPEC (Mahin and Lin 1983). Normalized strength factors are defined as

$$\eta = \frac{R_y}{ma_{max}} \dots \dots \dots (15)$$

where a_{\max} = the peak ground acceleration of a particular earthquake record; R_y = the yield strength of the SDOF; and m = the mass of the equivalent SDOF system. For this study, ductility demand μ is defined as the maximum displacement, in absolute value, divided by the yield displacement. These steps were taken to ensure that the SDOF systems were insensitive to variations in ground motion intensity. All final ductilities for the SDOF benchmark systems were within 10% or less of their targeted ductilities, when analyzed with the program used for the torsionally coupled systems.

3. The equivalent SDOF systems were then reanalyzed elastically, using the respective earthquake excitations scaled to levels that produced the desired target ductilities in the nonlinear systems ($a_{\max} = 4\pi^2\delta_y/T^2\eta$).

4. The torsionally coupled systems were first analyzed elastically. The earthquake was scaled for each parametric case, so that the torsionally coupled system's weak (more flexible) element maximum elastic displacement response would equal that of the equivalent elastic SDOF system.

5. Using the new earthquake scalings found in the previous step, the inelastic responses of the torsionally coupled systems were calculated, and the ductility demands were calculated for each element.

6. The ductility factors calculated for each individual torsionally coupled case analyzed were then divided by the ductility factors obtained from their respective equivalent inelastic SDOF system, to obtain a ratio of the ductilities (indicated as "ductility amplification ratios" on all figures herein). This ratio is independent of the selected target ductilities. The ductility amplification ratios for each element of the two-element systems appeared to provide the best quantitative measure of the damage sensitivity of the systems.

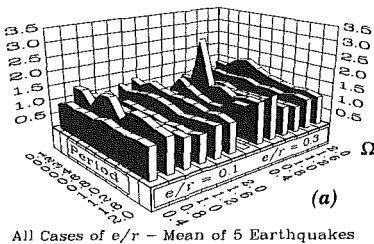
Response analyses for the torsionally coupled systems were performed using the general nonlinear dynamic analysis program ANSR-1 (Mondkar and Powell 1975). The time step used in the time history analyses using ANSR was chosen to be at least less than $T/30$ of the smallest of the two true periods of each system, but never smaller than 0.002 s or larger than 0.02 s.

Results of Parametric Study and Observations

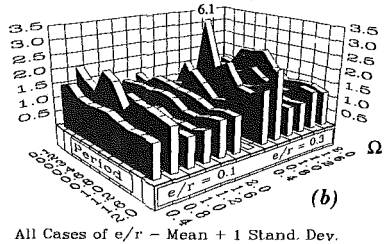
Figs. 5–7 present the results from the aforementioned step 6. These plots show the mean and mean-plus-one standard-deviation ductility amplification ratios of the weak (Fig. 5) and strong (Fig. 6) elements for a target ductility of 4, followed by the same information for weak elements for a target ductility of 8 (Fig. 7) for the five earthquake records described.

By observing the results of those ductility amplification ratios, one may notice that, for the $\Omega = 1.0$ case, all weak element ductility amplification ratios are equal to 1.0 (i.e., weak element ductility demands are equal to the equivalent SDOF system ductility demands). The analytical demonstration that equal displacements must be observed for the case $\Omega = 1.0$, if the aforementioned procedure is followed, is presented in Bruneau and Mahin (1987).

These figures clearly show that the element ductility amplification ratios obtained by the method outlined are independent of the uncoupled periods (T_x), normalized eccentricities (e/r), target ductility (μ_T), and ratios of uncoupled frequencies (Ω). This means that the method is stable in providing a reliable estimate of the torsionally coupled system's element ductilities based on the concept of an equivalent SDOF system.

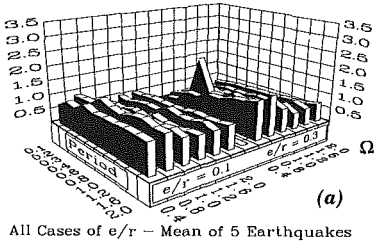


All Cases of e/r - Mean of 5 Earthquakes

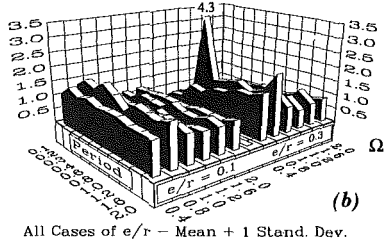


All Cases of e/r - Mean + 1 Stand. Dev.

FIG. 5. Weak Element Ductility Amplification Ratios for Target Ductility of 4: (a) Mean; and (b) Mean-Plus-One Standard Deviation (Five Earthquake Records)

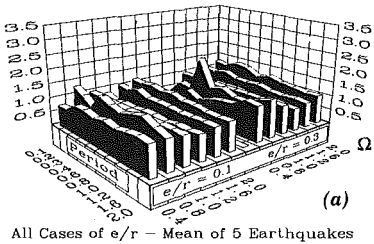


All Cases of e/r - Mean of 5 Earthquakes

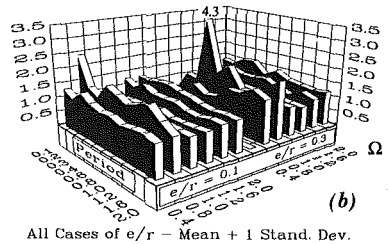


All Cases of e/r - Mean + 1 Stand. Dev.

FIG. 6. Strong Element Ductility Amplification Ratios for Target Ductility of 4: (a) Mean; and (b) Mean-Plus-One Standard Deviation (Five Earthquake Records)



All Cases of e/r - Mean of 5 Earthquakes



All Cases of e/r - Mean + 1 Stand. Dev.

FIG. 7. Weak Element Ductility Amplification Ratios for Target Ductility of 8: (a) Mean; and (b) Mean-Plus-One Standard Deviation (Five Earthquake Records)

The ductility amplification ratios calculated for individual earthquake records are, of course, a lot more variable than the one measured for the mean response for five earthquakes. Some very large values are obtained for particular combinations of parameters, but, as mentioned previously, no trends can be identified in the occurrence of those more sensitive combinations. The mean response from five earthquake excitations provides a meaningful indicator of the overall severity of the structural response.

The mean ductility amplification ratios remain relatively close to unity, only exceeding a value of 2.0 for the weak element when $T_x = 0.4$, $\Omega = 0.8$, and $(e/r) = 0.3$. This is a direct consequence of the unique extreme ductility amplification ratio that occurred for the Pacoima Dam earthquake

record for this particular combination of parameters. Should the Pacoima Dam contribution at this particular point be removed, the mean value would drop to 1.39 for target ductility of 4, and 1.05 for target ductility of 8. Other than this particular point of unusually high sensitivity, the mean weak element response exceeds 1.5 only in five of 120 occasions (the maximum value being 1.7). Considering the nature of ductility measurements in earthquake engineering and the accuracy desired in ductility predictions of this kind, element ductility amplification ratios of 1.25 or less might not be considered significant, ductility amplification ratios from 1.25 to 1.5 might be considered of moderate importance, and ratios above 1.5 might be judged to be of major importance. Following this arbitrary convention, the observed discrepancies in ductility amplification ratios obtained from this method are mostly of moderate importance, or less.

In some cases, the proposed liaison overestimates ductility amplification ratios. Consistent with the previous characterization, ductility amplification ratios of 0.75 and less can be defined as being moderately significant. Results obtained for the weak element for $(e/r) = 0.3$ when $\Omega = 0.4$ and $T_x \leq 0.3$ and when $\Omega = 0.8$ and $T_x = 0.1$, for both target ductilities are thus moderately significant. Similar overconservatism is obtained for the strong elements on a regular basis (except, perhaps, for long periods and low e/r values). Some moderate conservatism in weak element response is infrequent. If the initially eccentric system in these particular cases had been excited to the same earthquake level needed to produce a ductility of 4 for the equivalent SDOF system (instead of scaling the earthquake, as was explained), the predicted responses would have been excessively unconservative. For example, for the N-S component of the 1940 El Centro record, the case $T_x = 0.1$, $\Omega = 0.4$, and $e/r = 0.3$, which resulted in a conservative ductility of 2 for target ductility of 4, would reach a ductility of 13.5, if the motion was not scaled by the proposed method. As far as the strong elements are concerned, low-ductility amplification ratios are not regarded negatively. It is nevertheless noteworthy that some strong element ductility amplification ratios are extremely low, especially for systems with short periods and high (e/r) ratios.

If the previous methodology is followed, a maximum mean value of weak element ductility amplification ratio of 1.5, and a maximum mean strong element ductility amplification ratio of 1.0 would be conservatively expected. When $\Omega = 1$, a weak element ductility amplification ratio of 1 would be expected. Mean-plus-one standard-deviation results are presented to illustrate the often large dispersion of the results. Following the methodology previously outlined, a weak element ductility amplification ratio of 2.0 (except for the special case of $\Omega = 1$, where a ratio of 1 is again expected), and a strong element ductility amplification ratio of 1.0 when $\Omega \geq 1.0$ (and 1.5 otherwise) appear to be the maximum values to expect in this case. Again, these mean-plus-one standard-deviation values were obtained from only five earthquake records.

EXTENSION OF INVESTIGATION TO MORE ELABORATE CASE STUDIES

The aforementioned results and observations were obtained from relatively simple structural systems and element models. In this section, some more complex structures were investigated to verify whether these previous findings remain valid. Rather than repeating a comprehensive parametric study

for many complex systems and all the possible variables, a case-study approach was adopted to investigate the effect of each level of complication individually, using a common reference case as a benchmark when possible.

All the following single-story cases have an uncoupled translational period of $T_x = 0.4$ s and a normalized eccentricity (e/r) of 0.3. They were subjected to the N-S component of the 1940 El Centro earthquake scaled to produce a target ductility of 4 on the equivalent SDOF systems. Six values of Ω (0.4, 0.8, 1.0, 1.2, 1.6, and 2.0) were used in each case studied.

Single-Story Multielement Systems

Previously, only two-element systems were considered. While this is not an uncommon structural system, it was conjectured that results obtained might be overly conservative when applied to systems with more load-resisting elements. Systems with four and six regularly spaced elements were considered. Various stiffness distributions between the elements were considered. Systems with linear variation of stiffness were first studied with three different regular geometric distributions for systems with four lateral-load-resisting element systems, and one distribution for systems with six lateral-load-resisting elements. Then, single-step and double-step stiffness variations were studied on systems with four lateral-load-resisting elements. For the single-step variation, elements on a given side of the center of mass have the same stiffness (different from that of the other side), whereas for the double-step variation, one outside element was set to a high stiffness value, the other one to a low stiffness value, and inside elements shared the same median value. Finally, a single four-element case of totally irregular stiffness and geometric distribution was analyzed; the chosen configuration, illustrated in Fig. 8, represents a structure where the mass and stiffness variations along the length would be opposed, creating a rather severe case of eccentricity. Except for that last irregular configuration, multielement systems studied were geometrically symmetrical with respect to the center of mass, such that each element on one side of the center of mass had an equidistant counterpart, often of different stiffness, on the other side of this center. These multiple analyses were expected to cover a wide range of conceivable structures.

The previously described methodology was used to match the maximum elastic displacement of both the equivalent SDOF system and the eccentric system's weaker edge element to provide appropriate SDOF strength ratios, and the resulting edge element ductility amplification ratios were computed. As before, the equivalent SDOF element model was chosen to match the weak edge element.

Representative element ductility amplification ratios thus obtained are summarized in Table 1; D_1 and D_2 are the distance between the center of mass and the outside and inside lateral-load-resisting structural elements, respectively. Variations in the type of stiffness distribution do not appear to affect the ductility amplification ratios significantly; i.e., when compared to an equivalent SDOF system based on the previously explained method, the ductility amplification ratios seem to be consistent. Further, the number of elements does not appear to significantly affect the magnitude of the ductility amplification ratios. When compared to the reference two-element systems, an increase of about 25% in the ductility amplification ratio is the highest amplification observed for regularly spaced elements. For the totally irregular four-element system, the discrepancy with the reference system is somewhat greater.

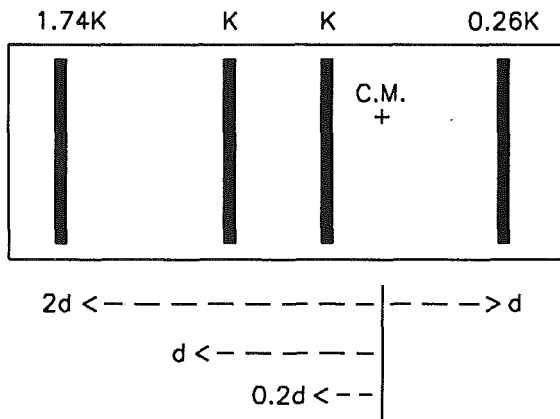


FIG. 8. Plan View of Totally Irregular Four-Element Single-Story System

TABLE 1. Lateral-Load-Resisting Element Ductility Amplification Ratios for Initially Eccentric Multielement Systems Having $(e/r) = 0.3$ and $T_x = 0.4$ s

System characteristics (1)		Ω					
		0.4 (2)	0.8 (3)	1.0 (4)	1.2 (5)	1.6 (6)	2.0 (7)
(a) Reference Two-Element System							
Weak element		0.83	0.78	1.00	0.89	1.53	1.88
Strong element		1.06	0.98	0.93	0.48	0.38	0.53
(b) Four-Element System with Linear Stiffness Variation							
Weak element	$D_1/D_2 = 2$	0.74	0.74	1.07	0.83	1.20	1.68
	$D_1/D_2 = 3$	—	0.75	1.15	0.77	1.18	1.56
	$D_1/D_2 = 4$	—	0.82	1.22	0.75	1.17	1.53
Strong element	$D_1/D_2 = 2$	1.09	1.07	0.87	0.46	0.35	0.54
	$D_1/D_2 = 3$	—	1.06	0.82	0.44	0.32	0.51
	$D_1/D_2 = 4$	—	1.05	0.85	0.41	0.31	0.49
(c) Four-Element System with Step Stiffness Variation							
Weak element	Single step	0.68	0.72	1.05	0.83	1.20	1.66
	Double step	—	0.76	1.10	0.82	1.20	1.71
Strong element	Single step	1.10	1.06	0.86	0.47	0.35	0.54
	Double step	—	1.06	0.89	0.45	0.35	0.54
(d) Six-Element System with Linear Stiffness Variation							
Weak element		—	0.74	1.26	0.75	1.18	1.53
Strong element		—	1.06	0.90	0.44	0.30	0.52
(e) Totally Irregular Four-Element System (One Case)							
Weak element		1.14	—	—	—	—	—
Strong element		1.02	—	—	—	—	—

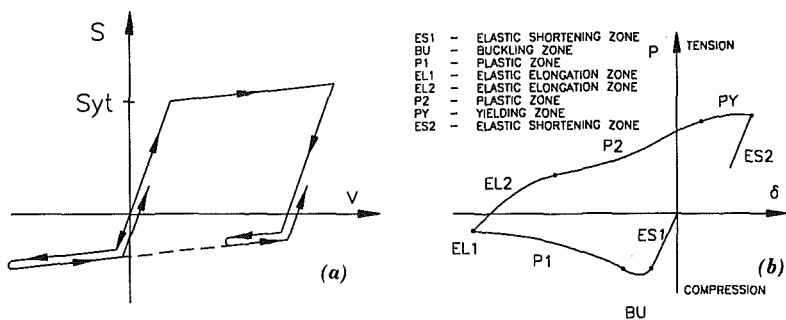


FIG. 9. Models: (a) Inelastic Truss Element Model with Elastic Buckling (Yielding in Tension, Buckling in Compression); and (b) Physical Brace Element Model

Various Element Models—Single-Story Systems

Up to this point, all analyses were conducted using a bilinear hysteretic model with 0.5% strain hardening. Other element models will now be considered to determine how the previous findings would be affected. To this end, two different models were chosen to reflect the complex hysteretic behavior associated with braced frames.

1. A simple brace model [Fig. 9(a)] that allows yielding in tension and elastic buckling in compression (Mondkar and Powell 1975).
2. A more complex physical brace model [Fig. 9(b)] that is capable of better representation of the true behavior of braces (Mahin and Ikeda 1984).

All structural elements consisted of pairs of elements oriented to represent X-braced frames, without braces connections at their midpoints. As before, the torsionally coupled results are compared with an equivalent SDOF system having an identical element model so that the true contribution of the coupling can be extracted. This is important, because braced frames can be more sensitive than bilinear hysteretic systems (in some cases, the physical brace element was found to reach displacement ductilities of more than 10 times those attained with the bilinear hysteretic model under the same level of earthquake excitation). In consequence, the equivalent SDOF system force-displacement relationship was selected to be identical to the one for the weak element in the coupled system, and was subjected to a different level of earthquake excitation so that its elastic displacement matched that of the weak element in the coupled system.

For the elastic buckling brace element model, various combinations of compression and tension yield strengths were investigated. In each case, the sum of those yield strengths was selected to be identical. Three yield combinations were investigated. From Table 2, the previously outlined methodology applied to the new element model appears to preserve the parametric insensitivity observed for simpler systems. Results are even more clustered around the ductility amplification ratio of 1 than for the reference two-element hysteretic system for this particular set of parameters.

For systems with physical brace model used for the X-braced frames, only two yield combinations were investigated: the "yield = $1.25F_y$, buckling = $0.75F_y$ case," and the "yield = $1.5F_y$, buckling = $0.5F_y$ case," which corresponded to intermediate ($KL/r = 103$) and large ($KL/r = 128$) slender-

TABLE 2. Lateral-Load-Resisting Element Ductility Amplification Ratios for Initially Eccentric Braced-Frame Systems with $(e/r) = 0.3$ and $T_x = 0.4$ s

System characteristics (1)	Y (2)	B (3)	Ω					
			0.4 (4)	0.8 (5)	1.0 (6)	1.2 (7)	1.6 (8)	2.0 (9)
(a) Reference Two-Element System with Bilinear Model								
Weak element			0.83	0.78	1.00	0.89	1.53	1.88
Strong element			1.06	0.98	0.93	0.48	0.38	0.53
(b) Elastic Buckling Element Model								
Weak element	1.00	1.00	0.59	0.98	1.00	0.79	1.45	1.20
	1.25	0.75	0.85	1.04	1.00	0.74	0.99	0.99
	1.50	0.50	0.71	1.00	1.00	0.76	1.08	1.09
Strong element	1.00	1.00	0.61	0.43	0.24	0.22	0.30	0.26
	1.25	0.75	0.95	0.32	0.27	0.20	0.32	0.30
	1.50	0.50	0.63	0.69	0.37	0.20	0.38	0.35
(c) Physical Brace Element Model								
Weak element	1.25	0.75	0.73	0.48	1.00	0.89	1.39	1.82
	1.50	0.50	0.71	0.83	1.00	0.61	1.60	1.56
Strong element	1.25	0.75	0.87	0.78	0.91	0.47	0.27	0.25
	1.50	0.50	0.81	0.80	0.78	0.85	0.99	0.60

Note: Y = yield level in proportion to specified yield stress F_y . B = buckling level in proportion to specified yield stress F_y .

ness, with both elements of the X-braced system having the same slenderness. Results are presented in Table 2, and again, they are comparable to what was previously obtained for the bilinear hysteretic model.

Multistory Systems

One of the major problems associated with multistory systems is the definition and determination of the centers of rigidity. A good treatment of this topic can be found in Cheung and Tso (1986). Nevertheless, for the purpose of this study, the centers of rigidity were not essential to perform the ensuing examples, and thus were not identified.

For the following case studies, all elements were modeled as being bilinear hysteretic with 0.5% strain hardening. Rayleigh damping of 2% was chosen at the first and last period of the multistory system, which implies that the intermediate periods had a somewhat lower damping.

No target ductility was fixed for the equivalent SDOF systems in these analyses. Various ductility definitions will be used hereafter, and it was judged more appropriate to simply apply the N-S component of the 1940 El Centro earthquake, with peak acceleration scaled to 0.5 g, to the multistory systems of interest. This approach is reasonable, as the ductility amplification ratios of torsionally coupled systems were demonstrated to be independent of the target level of excitation.

The responses of multistory torsionally coupled systems and equivalent SDOF systems were compared in hope of extending the validity of the concepts derived for the single-story systems. As done previously, the equivalent SDOF system's period was defined as that of the first dominantly trans-

lational mode of the multistory system. Unfortunately, for many multistory systems, it may be particularly difficult to visually recognize this mode. The following equations allow a formal determination of the mode shape identification factor (percentage of torsional or rotational) in each direction. (Some commercially available structural analysis programs automatically provide this information when performing modal analysis.)

For a system with normalized mode shapes such that

$$\Phi_N^T m \Phi_N = M_N = 1 \dots \dots \dots (16)$$

the expression for the "effective modal participation factors" can be expanded into

$$\frac{\Phi_N L_N}{M_N} = \Phi_N L_N = \Phi_N \Phi_N^T m \mathbf{r}^* \dots \dots \dots (17)$$

where \mathbf{r}^* = the pseudostatic influence-coefficient vector. Using the equations derived around the center of mass (Eqs. 1 and 2), m_i being the terms of the diagonal mass matrix, the mode shape identification factors can be obtained by summing the diagonal elements of the $(\Phi_N \Phi_N^T m)$ matrix, such that

$$\sum_{i=1}^N \Phi_{iN}^2 m_i = \Phi_{1N}^2 m_1 + \Phi_{2N}^2 m_2 + \dots + \Phi_{iN}^2 m_i + \Phi_{jN}^2 (mr_j^2) + \Phi_{(j+1)N}^2 [mr_{(j+1)}^2] + \dots + \Phi_{NN}^2 (mr_N^2) \dots \dots \dots (18)$$

where the translational mass terms are grouped separately from the mass moment of inertia terms. The highest period for which the grouped translational terms equal or exceed 50% of the sum is defined as the equivalent period (an exact 50% split is typical of systems with $\Omega = 1$).

An additional problem comes from the impossibility of finding an SDOF element model that would perfectly match at all times the behavior of the weak side of an initially eccentric multistory system. Even if δ_i is set to each level's interstory yield displacement, these are not necessarily reached simultaneously during dynamic response of this system. Nevertheless, it was decided to model the SDOF system as a bilinear system with yield displacement equal to the sum of the multistory system's interstory yield displacements. In light of the general goals pursued in this section, that simplification was considered to be acceptable. Three types of two-story systems were used in this part of the study, each described in the following.

Multistory Systems with Regular Configuration

Systems with regular configuration were simply defined here as systems for which the floor plan remained the same for each story (equal mass and mass moment of inertia) and where the reduction in stiffness from story to story remained proportional for each lateral-force-resisting structural element. Monosymmetric systems having two lateral-load-resisting structural elements per story were selected for the study.

Since the location of the center of stiffness had not been identified, there was no attempt to define a ratio of uncoupled frequencies Ω for multistory systems. Instead, it was decided to conserve the same strong-to-weak element stiffness ratio as for the cases of two-element systems studied. For two-element single-story systems having $(e/r) = 0.3$ and $\Omega = 0.4, 0.8, 1.0, 1.2, 1.6,$ and 2.0 , these stiffness ratios were 7.0, 2.2, 1.86, 1.67, 1.46, and

TABLE 3. Lateral-Load-Resisting Element Ductility Amplification Ratios for Two-Story Initially Eccentric Systems: Interstory and Roof Element Ductility Amplification Ratios

System characteristics (1)		Strong/Weak Stiffness Ratio					
		7.00 (2)	2.20 (3)	1.86 (4)	1.67 (5)	1.46 (6)	1.35 (7)
(a) $K_{top}/K_{bot} = 2/3$							
Weak element	Interstory 0-1	0.57	2.36	1.35	1.33	1.75	1.83
	Interstory 1-2	0.45	0.95	0.82	0.39	0.51	0.53
	Roof total	0.36	1.57	0.79	0.83	0.87	0.94
Strong element	Interstory 0-1	0.33	0.69	0.61	0.30	0.39	0.52
	Interstory 1-2	0.35	1.28	0.50	0.33	0.16	0.20
	Roof total	0.19	0.84	0.49	0.31	0.24	0.34
(b) $K_{top}/K_{bot} = 1/3$							
Weak element	Interstory 0-1	0.41	0.67	0.50	0.24	0.28	0.27
	Interstory 1-2	0.77	3.14	2.05	1.32	2.52	3.28
	Roof total	0.39	1.72	0.98	0.66	1.26	1.67
Strong element	Interstory 0-1	0.09	0.25	0.13	0.10	0.17	0.20
	Interstory 1-2	0.55	2.52	1.08	0.81	0.81	0.53
	Roof total	0.29	1.26	0.56	0.43	0.45	0.33

1.35, respectively. These stiffness ratios were adopted here and kept constant from story to story.

Two different variations of the stiffness from the first to the second story were investigated. In one case, the ratio of second story over first story stiffnesses was 2/3, and in the other case 1/3. The corresponding two uncoupled translational periods were 0.28 and 0.12 s for the first case, and 0.34 and 0.14 s for the second case.

To perform the proper ductility comparison, it was consistent with the previous methodology to match the maximum elastic displacement of the equivalent SDOF system with the maximum elastic roof displacement on the weak side of the multistory system.

Maximum inter-story drifts and corresponding interstory displacement ductilities were also calculated for each element. The roof displacement ductilities as well as each inter-story displacement ductilities were divided by the ductility of the equivalent SDOF system, providing three different ductility amplification ratio indicators. These are tabulated in Table 3 for the weak and strong elements. Note that roof yield displacement was simply defined as the sum of each story's element yield displacement.

Table 3 shows that the roof ductility amplification ratios, although different from what has generally been obtained for two-element systems, are not necessarily better or worse—most results being conservative or slightly above unity with a few occasionally larger values. This is remarkable, considering the approximations in the equivalent SDOF model as well as the nonuniformity of damping in all modes.

Unfortunately, the inter-story ductility amplification ratios did not fare as well. For the case when the ratio of second story over first story stiffnesses was 2/3, the lower story's inter-story ductility amplification ratios tended to be rather large, whereas all those of the upper story ones were conser-

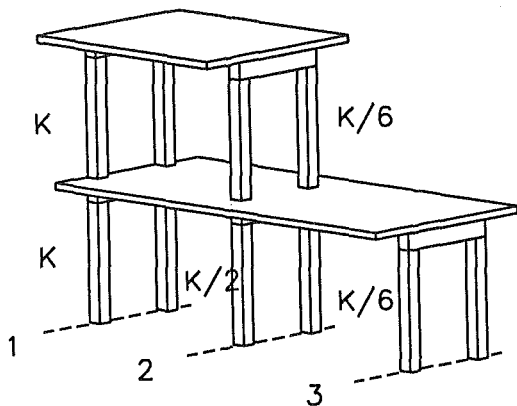


FIG. 10. Two-Story System with Irregular Configuration

vative. For the case where the second to first story ratio of stiffnesses was $1/3$, the situation was reversed, as the top story ductility amplification ratios were considerably high.

Clearly, the equivalent SDOF system analogy appears promising to predict roof displacement ductilities, but somewhat deficient when inelastic action tends to concentrate in a given story. This same phenomenon also occurs when comparing inelastic response of planar multistory frames (without torsional coupling) with inelastic SDOF systems. More research on this topic is needed.

Multistory Systems with Irregular Configuration

One severely irregular configuration, consisting of a single two-story structure with a setback, was analyzed. The top slab had one-half the floor area (and mass) of the lower slab and, consequently, a five-times-lesser mass moment of inertia. Both floors were assumed to be infinitely rigid in their plan.

Severe stiffness variations were chosen to accentuate the coupling. The structure, still monosymmetric, is schematically illustrated in Fig. 10. The lateral resisting elements were located on three equally spaced design lines on the lower floor, and two on the top floor. The stiffness on the first design line (the common edge to both stories) was set to be the largest and uniform along height. Referring to the inter-story stiffness along the first design line as K , then the stiffness along the second design line was taken to be $K/2$ on the lower story, and $K/6$ on the top story, and again $K/6$ on the third design line. All elements were assigned similar yield displacement in accordance with the bilinear hysteretic model previously defined in this study. The first two periods (0.6 and 0.4 s) were dominantly rotational, and the last two (0.18 and 0.082 s) were dominantly translational. The equivalent SDOF system period was thus taken as 0.18 s.

With such an irregular system, it is not obvious which maximum elastic displacement should be made to match the maximum elastic displacement of the SDOF system. Here, a weaker side can fortunately be identified, but this may not be possible for other structural configurations. Judgment will generally be needed, especially for unusual setback structures where the largest elastic edge displacement could occur on a lower story. In the current

TABLE 4. Lateral-Load-Resisting Element Ductility Amplification Ratios for Two-Story Initially Eccentric Systems with Irregular Configuration

System characteristics (1)	1 (2)	2 (3)	3 (4)
Interstory ductility amplification ratios			
Ground to first story	1.58	0.74	1.76
First story to roof	0.31	1.33	—
Roof total ductility amplification ratios	0.92	0.49	—

example, the roof weak side maximum displacement was used for the comparison. Other steps of the methodology were executed as before, and the results are presented in Table 4.

No general conclusions should be drawn on the results of this single case, but it is noteworthy that while the roof displacement ductility amplification ratios were conservative to good, the inter-story ductility amplification ratios were definitely worse. Nevertheless, considering the severe irregularity of this sample structure, the resulting ductility amplification ratios remain reasonably well behaved, the maximum value being 1.76.

PREDICTION OF TORSIONAL RESPONSE

Obviously, the concept of an equivalent SDOF system can be potentially very useful in design. Although there apparently is no easy way to obtain an exact match of the weak element displacement with a meaningful equivalent SDOF system for all values of Ω , the proposed method can provide a relatively accurate prediction of the initially eccentric system's element ductility demand, as shown in the preceding section. The use of the equivalent SDOF system procedure, in a design approach, to estimate the inelastic response of torsionally coupled systems will now be illustrated.

A design engineer using dynamic elastic analysis tools (like the elastic response spectrum method or time history analysis) may easily calculate the elastically predicted response for the weak element. It is assumed, for simplicity in this example, that the calculation is performed for a single ground motion. This calculated elastic response is to be denoted R_{weak} .

The elastic response of the equivalent SDOF system can be obtained from an SDOF elastic response spectrum (readily available for most earthquake records); let this SDOF response be called R_{SDOF} . To match the elastic responses of the weak element and the equivalent SDOF system, the earthquake applied to the equivalent SDOF system should be scaled by R_{weak} / R_{SDOF} .

It is now possible to obtain a prediction of the ductility demand on the equivalent SDOF system subjected to this corrected earthquake level by consulting inelastic response spectra (Mahin and Lin 1983). These spectra are relatively straightforward to calculate, using standard numerical analysis procedures, and need only be constructed once for each combination of earthquake, damping, and element model. Single earthquake or multiple earthquake spectra can also be constructed. Of course, the element model for the SDOF must match the one for the elements of the torsionally coupled system.

It is then straightforward to calculate the strength factor, defined as η , and read the ductility demand for this equivalent SDOF system off the inelastic

response spectrum. If $\Omega = 1$, this equivalent SDOF system's ductility demand can be assumed to be equal to both the weak and strong element ductilities of the torsionally coupled system; otherwise, a conservative weak element ductility should be estimated as possibly 50% larger. This guideline is based on the mean ductility amplification ratios previously obtained for five earthquake records.

Example

An initially eccentric two-element structure having the response parameters $T_x = 0.2$ s, $\Omega = 2$ and $e/r = 0.1$ is analyzed. For this system, the two true periods are $T_1 = 0.20$ s and $T_2 = 0.10$ s. The element model is bilinear with 0.5% strain hardening, and damping is 2% of critical. The yield displacement of this system is taken to be $\delta_y = 0.12$ in. (3.05 mm). The 1940 El Centro earthquake (N-S component) was scaled to a peak acceleration of 0.46 g and an elastic dynamic time-history analysis was performed; the resulting edge displacement for the weak element was 0.50 in. (12.7 mm).

Then, using an elastic response spectrum for this earthquake component that had an actual recorded peak acceleration of 0.348 g, the pseudodisplacement for the equivalent SDOF system (with period $T_{SDOF} = 0.20$ s) was found to be $Sd = 0.36$ in. (9.15 mm). To match the weak element elastic displacement with the equivalent SDOF system, the earthquake used in the

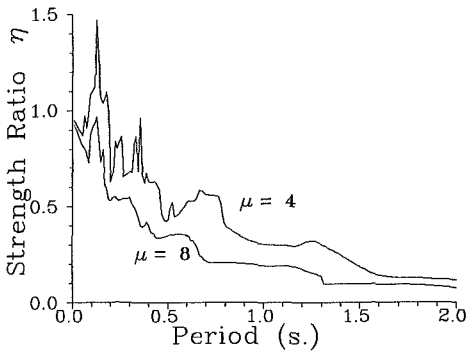
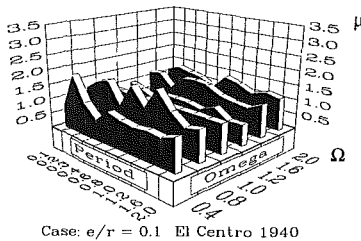


FIG. 11. Constant Ductility Response Spectra for NS Component of El Centro 1940 Earthquake, Bilinear Element Model with 0.5% Strain Hardening, 2% Damping, and Displacement Ductilities of 4 and 8



Case: $e/r = 0.1$ El Centro 1940

FIG. 12. Weak Element Ductility Amplification Ratios for Target Ductility of 4 and El Centro 1940 NS Earthquake Record

equivalent SDOF concept must be scaled as

$$\frac{\text{weak element displacement}}{Sd \text{ from equivalent SDOF}} = \frac{0.50}{0.36} = 1.39 \dots \dots \dots (19)$$

Therefore, the peak acceleration for this equivalent SDOF increases by 1.39 and becomes 0.483 g (187 in./sq sec, or 4.75 m/s²), and using the same yield displacement of 0.12 in. (3.05 mm) for the equivalent SDOF system, the strength level can be estimated by

$$\eta = \frac{R_y}{ma_{\max}} = \frac{K\delta_y}{ma_{\max}} = \omega_{SDOF}^2 \frac{\delta_y}{a_{\max}} = 987 \frac{(0.12)}{187} = 0.64 \dots \dots \dots (20)$$

Finally, reading from the constant ductility response spectra of Fig. 11 (which has been derived for two ductility levels, 2% damping and bilinear model with 0.5% strain hardening), one can see that for a period of 0.20 s and a strength ratio of 0.64, the ductility demand on the equivalent SDOF system is approximately 4. Since Ω is not equal to unity, it is appropriate to increase by 50% the predicted weak element value, and use directly the obtained SDOF ductility as an estimate of the strong element value. The estimated weak element ductility is then 6, and the estimated strong element ductility remains 4. This is adequate, as the calculated weak and strong element ductilities for the initially eccentric system are respectively 5.2 and 3.0 (Fig. 12). To illustrate the methodology, only one earthquake excitation was used. In a true design procedure, it is essential that many earthquake records be included.

CONCLUSIONS

Many torsionally coupled systems were analyzed and compared with equivalent SDOF systems to investigate the effect of various parameters on the response of their lateral-load-resisting elements. A methodology, proposed to perform a meaningful liaison between the equivalent SDOF system and corresponding torsionally coupled system, provided a reliable way to predict the inelastic response of structural elements. The ratio of ductilities obtained using the proposed method were unaffected by changes in the level of excitation (target ductility level), ratio of uncoupled frequencies Ω , uncoupled period T_x , and normalized eccentricities (e/r). A number of other analyses suggest that these ratios were also unaffected by the number of lateral-load-resisting elements used, as well as the type of inelastic element model adopted.

In the case of $\Omega = 1.0$, the equivalent SDOF response will perfectly match the weak element response of the torsionally coupled system, provided that the inelastic element force-displacement relationships are similar; that is, yield displacements, damping, and strain-hardening values are similar in the case of bilinear models.

For other values of Ω , the ductility amplification ratios obtained by the proposed equivalent SDOF method, following the methodology explained in the previous section, were often close to unity in the case of mean response from five earthquake excitations, with a conservative design value to be taken as 1.5. Of course, response under a single earthquake excitation may differ strongly from the one predicted using the mean response from five earthquakes, the same way this can also be expected in the case of symmetrical structures.

An easy design procedure, relying mainly on elastic analysis and readily available design tools, can be used to obtain good estimates of element ductilities for simple torsionally coupled systems. Some studies of more complex multistory systems indicate that the suggested approach is promising and deserves additional consideration in future research.

ACKNOWLEDGMENTS

This research program was supported by the National Science Foundation. This support is sincerely appreciated. The findings and recommendations in this paper, however, are those of the writers and not necessarily those of the sponsor.

APPENDIX I. REFERENCES

- Anagnostopoulos, S. A., Roesset, J. M., and Biggs, J. M. (1973). "Nonlinear dynamic analysis of buildings with torsional effects." *Fifth World Conf. on Earthquake Engrg.*, 2, Rome, Italy, 1822-1825.
- Bozorgnia, Y., and Tso, W. K. (1986). "Inelastic earthquake response of asymmetric structures." *J. Struct. Engrg.*, ASCE, 112(2), 383-400.
- Bruneau, M., and Mahin, S. A. (1987). "Inelastic response of structures with mass or stiffness eccentricities in plan." *Report No. EERC 87-12*, Earthquake Engrg. Res. Ctr., Univ. of California, Berkeley, Calif., Sep.
- Cheung, V. W.-T., and Tso, W. K. (1986). "Eccentricity in irregular multistory buildings." *Canadian J. Civ. Engrg.*, 13(1), 46-52.
- Clough, R. W., and Penzien, J. P. (1975). *Dynamics of structures*. McGraw-Hill, Inc., New York, N.Y.
- Kan, C. L., and Chopra, A. K. (1979). "Linear and nonlinear earthquake responses of simple torsionally coupled systems." *Report No. EERC 79-03*, Earthquake Engrg. Res. Ctr., Univ. of California, Berkeley, Calif., Feb.
- Mahin, S. A., and Lin, J. (1983). "Construction of inelastic response spectra for single-degree-of-freedom systems." *Report No. EERC 83-17*, Earthquake Engrg. Res. Ctr., Univ. of California, Berkeley, Calif., Jun.
- Mahin, S. A., and Ikeda, K. (1986). "A refined physical theory model for predicting the seismic behavior of braced steel frames." *The Mexico Earthquake of 1985—Proc. Int. Conf.*, ASCE, Mexico City, Mexico, 308-327.
- Meli, R. (1986). "Evaluation of performance of concrete buildings damaged by the September 19, 1985, Mexico earthquake." *The Mexico Earthquake of 1985—Proc. Int. Conf.*, ASCE, Mexico City, Mexico, 308-327.
- Mitchell, D., et al. (1986). "Lessons from the 1985 Mexican earthquake." *Canadian J. Civ. Engrg.*, 13(5), 535-557.
- Mondkar, D. P., and Powell, G. H. (1975). "ANSR-1—General purpose program for analysis of nonlinear structural response." *Report No. EERC 75-37*, Earthquake Engrg. Res. Ctr., Univ. of California, Berkeley, Calif., Dec.
- Syamal, P. K., and Pekau, O. A. (1985). "Dynamic response of bilinear asymmetric structures." *Int. J. Earthquake Engrg. Soil Dyn.*, 13, 527-541.
- Tsincias, T. G., and Hutchinson, G. L. (1981). "Evaluation of code requirements for the earthquake resistant design of torsionally coupled buildings." *Proc. Inst. Civ. Engrs.*, 71, Part 2, 821-843.
- Tso, W. K., and Sadek, A. W. (1984). "Inelastic response of eccentric buildings subjected to bi-directional ground motions." *Eighth World Conf. Earthquake Engrg.*, San Francisco, Calif., 203-210.
- Yamazaki, Y. (1986). "Inelastic torsional response of structures subjected to earthquake ground motions." *Report No. EERC 80-07*, Earthquake Engrg. Res. Ctr., Univ. of California, Berkeley, Calif., Apr.

APPENDIX II. NOTATION

The following symbols are used in this paper:

a_{\max}	=	peak ground acceleration;
D_1	=	distance from center of mass to outside element in multielement systems;
D_2	=	distance from center of mass to inside element in multielement systems;
E	=	elastic modulus of elasticity;
$EDMPF$	=	edge displacement modal participation factor;
e	=	static plan eccentricity of floor;
(e/r)	=	normalized eccentricity of floor;
F_y	=	yield stress;
g	=	gravitational constant;
K_{BOT}	=	lateral stiffness of bottom story;
K_{ix}	=	translational stiffness of element i in x -direction;
K_{TOP}	=	lateral stiffness of top story;
K_x	=	translational stiffness of floor in x -direction;
K_θ	=	rotational stiffness of structure defined at center of mass;
M_N	=	generalized mass of n th normal mode;
m	=	mass of floor;
R_y	=	yield strength;
r	=	radius of gyration of floor;
\mathbf{r}^*	=	pseudostatic influence coefficient vector;
S_d	=	spectral displacement;
T_N	=	true period for n th natural mode;
T_x	=	uncoupled translational period;
T_θ	=	uncoupled rotational period;
\ddot{v}_{gx}	=	ground acceleration;
v_x	=	translational displacement of center of mass;
\ddot{v}_x	=	translational acceleration of center of mass;
v_θ	=	rotational displacement of floor around vertical axis;
\ddot{v}_θ	=	rotational acceleration of floor around vertical axis;
y_i	=	distance from element i to center of mass;
δ_y	=	yield displacement;
η	=	strength factor;
μ	=	displacement ductility;
μ_T	=	target displacement ductility;
ξ_N	=	damping for n th natural mode;
Φ_N	=	mode shape for n th natural mode;
Φ_{Ni}	=	component of mode shape for n th natural mode;
$\omega_{N(N=1,2)}$	=	true frequency for n th natural mode;
ω_x	=	uncoupled translational frequency; and
Ω	=	ratio of uncoupled frequency.